



## The interacting rotifer-biopolymers are anti- and disaggregating agents for human-type beta-amyloid *in vitro*

Zsolt Datki<sup>a,\*</sup>, Evelin Balazs<sup>a</sup>, Bence Galik<sup>b,c</sup>, Rita Sinka<sup>d</sup>, Lavinia Zeitler<sup>a</sup>, Zsolt Bozso<sup>e</sup>, Janos Kalman<sup>a</sup>, Tibor Hortobagyi<sup>f,g,1</sup>, Zita Galik-Olah<sup>a,1</sup>

<sup>a</sup> Department of Psychiatry, Albert Szent-Györgyi Medical School, University of Szeged, Korányi fasor 8-10, H-6725 Szeged, Hungary

<sup>b</sup> Bioinformatics Research Group, Bioinformatics and Sequencing Core Facility, Szentágotthai Research Centre, University of Pécs, Ifjúság u. 20, H-7624 Pécs, Hungary

<sup>c</sup> Department of Clinical Molecular Biology, Medical University of Białystok, ul. Jana Kilinskiego 1, 15-089 Białystok, Poland

<sup>d</sup> Department of Genetics, Faculty of Science and Informatics, University of Szeged, Közép fasor 52, H-6726, Hungary

<sup>e</sup> Department of Medical Chemistry, Albert Szent-Györgyi Medical School, University of Szeged, Semmelweis u. 6, H-6725 Szeged, Hungary

<sup>f</sup> Department of Pathology, Albert Szent-Györgyi Medical Center, University of Szeged, Állomás u. 1., H-6725 Szeged, Hungary

<sup>g</sup> Department of Old Age Psychiatry, Institute of Psychiatry Psychology & Neuroscience, King's College London, Box PO70, De Crespigny Park, Denmark Hill, SE5 8AF London, UK

### ARTICLE INFO

**Keywords:**  
Monogonant  
Rotifer  
Biopolymer  
beta-amyloid  
Aggregation  
*Euchlanis dilatata*

### ABSTRACT

Neurodegeneration-related human-type beta-amyloid 1-42 aggregates (H-A $\beta$ ) are one of the biochemical markers and executive molecules in Alzheimer's disease. The exogenic rotifer-specific biopolymer, namely Rotimer, has a protective effect against H-A $\beta$  toxicity on *Euchlanis dilatata* and *Lecane bulla* monogonant rotifers. Due to the external particle-dependent secreting activity of these animals, this natural exudate exists in a bound form on the surface of epoxy-metal beads, named as Rotimer Inductor Conglomerate (RIC). In this current work the experiential *in vitro* molecular interactions between Rotimer and A $\beta$ s are presented. The RIC form was uniformly used against H-A $\beta$  aggregation processes in stagogram- and fluorescent-based experiments. These well-known cell-toxic aggregates stably and quickly (only taking a few minutes) bind to RIC. The epoxy beads (as carriers) alone or the scrambled version of H-A $\beta$  (with random amino acid sequence) were the ineffective and inactive negative controls of this experimental system. The RIC has significant interacting, anti-aggregating and disaggregating effects on H-A $\beta$ . To detect these experiments, Bis-ANS and Thioflavin T were applied during amyloid binding, two aggregation-specific functional fluorescent dyes with different molecular characteristics. This newly described empirical interaction of Rotimer with H-A $\beta$  is a potential starting point and source of innovation concerning targeted human- and pharmaceutical applications.

### 1. Introduction

Various neurotoxic peptides (e.g., beta-amyloids) or proteins (e.g., alpha-synuclein, huntingtin and prion) are involved in the development of neurodegenerative diseases, where the aggregation is caused by an abnormal conformational change in related molecules [1]. These dysfunctions occur either extra- or intracellularly [2,3]. Several types of cell-toxic aggregates are known depending on different cognitive diseases [4], such as Alzheimer's disease (AD), characterized by human-type beta-amyloid 1-42 (H-A $\beta$ ) deposits in the brain [5].

The aggregating-mechanism of A $\beta$ s is influenced by different agents, which may have anti-aggregating and/or disaggregating effects.

Numerous studies have shown [6] that natural compounds (e.g., *Ginkgo biloba* extracts) have high pharmacological potentials and attenuating effects against the AD. Curcumin, besides its widespread positive effects, is another natural molecule that can also block the aggregation and is able to dissociate an existing one [7]. Various active substances with herbal origin show antagonistic effects against amyloid genesis activity and they may even have preventive and therapeutic relevance in dementias [8]. Some molecules (e.g., polyphenols or chaperones), in addition to inhibiting aggregation, can stabilize the native protein conformation [9]. Moreover, some anti-inflammatory small molecules (e.g., Aspirin) can also inhibit the aggregation processes, and significantly reverse the conformation of beta-sheet structures to alpha helix

\* Corresponding author.

E-mail address: [datki.zsolt@med.u-szeged.hu](mailto:datki.zsolt@med.u-szeged.hu) (Z. Datki).

<sup>1</sup> The authors contributed equally to this work (co-last authors).

<https://doi.org/10.1016/j.ijbiomac.2021.12.184>

Received 13 November 2021; Received in revised form 17 December 2021; Accepted 29 December 2021

Available online 7 January 2022

0141-8130/© 2022 The Authors.

Published by Elsevier B.V. This is an open access article under the CC BY-NC-ND license

(<http://creativecommons.org/licenses/by-nc-nd/4.0/>).

[10].

Various biopolymers emerged as new scientific possibilities in the research field and in the pragmatic application of natural agents. Based on their multifunctional roles in the living world, the question arises as to what impact they may have on aggregation processes. The answer can be investigated in an interdisciplinary approach connecting biotechnology with neurobiology. Since biopolymers are also involved in degradation processes in the natural habitat [11]; therefore, they may influence the conglomeration and aggregation processes. Several biopolymers affect the polymerization or precipitation of different types of organic materials and molecules [12]. Thus, preventing/inhibiting peptide or protein aggregation processes are also worth studying.

The secreting exudates had primarily been investigated with an industrial purpose; nevertheless, their beneficial effects have also been studied in medicine. A representative example for this technical translation is the gold nanoparticles, coated with dextrin or chitosan, which are able to inhibit insulin amyloid fibrillation in a complex form [13]. These biopolymer-coated particles interact with the insulin monomers and prevent the formation of its oligomers. The polysaccharide  $\beta$ -D-glucan and carboxymethylated derivatives were also able to block platelet aggregation [14]. In addition to various compounds, numerous proteins complexes (e.g., heat shock types) attenuate the aggregation of different monomers [15]. Because biopolymers are biocompatible, biodegradable and have low immunogenicity, they are promising theoretical sources in biomedicine [16], even in neurobiology. There are several natural molecules (e.g., collagen, gelatin, heparin or chitosan) that are the bases of artificial products available in clinical application [17]. Furthermore, many plant-based polymers (e.g., cellulose) can also be used as medical engineering constructs due to their good physical properties. These agents are suitable as therapeutic molecules in drug and gene delivery [18].

Based on basic- and preclinical research, Ow et al. [19] asserts that biomolecules play an increasing role in neuromedicine, related to the modulation of aggregation processes *in vitro*.

Some micrometazoans are able to produce exogenous biopolymers [20]. Of these phylogenetically conservative beings, the rotifers form large portion of natural water biomass; moreover, their possible application as modern *micro-in vivo* models have been demonstrated in several interdisciplinary areas, e.g., in pharmacotoxicology, neurobiology and especially in neurobiochemistry. Their exceptional ability for survival in neurotoxic aggregates-supplemented environment has been recently revealed [21]. This fact brings the rotifers into the attention of researchers committed to amyloid-related science. These animals are outstanding candidates for holistic and experiential studies investigating neurotoxic aggregates. Rotifer-specific biopolymer (namely Rotimer) was recently discovered and first described by Datki et al., [22] in academic literature. The production of *Euchlanis dilatata*- and *Lecane bulla*-specific Rotimers, as monogastric bioproducts, can be induced by mechanically stimulating these animals with various types of microparticles (e.g., carmine or urea crystals, epoxy beads and microcellulose). The multiple *in vitro* bioactivities of these biomolecules were proved by applying three different cell types: alga, yeast and human SH-SY5Y neuroblastoma. The exudates had no negative effect on the cells; however, they completely inhibited the motility and the proliferation of neuroblastoma cultures.

The effect of the Rotimer was further investigated on rotifers in terms of their viability, where the animals were treated with aggregated H-A $\beta$ . The H-A $\beta$  was non toxic to those native entities which were able to produce fiber webs; however, it proved to be harmful for Rotimer-depleted ones. In these experiments, the relations between biopolymer and H-A $\beta$  were indirectly tested *in vivo*. The potential interaction of Rotimer and H-A $\beta$  is directly investigated *in vitro* in animal-free conditions in this current study. Two different methods were applied to examine the potential Rotimer-A $\beta$ s connections: stagogram pattern analysis (interaction measurements) parallelly with fluorescence-based methods such as anti- and disaggregation monitoring. Stagogram

analysis is an adequate tool for quick and holistic evaluation of the possible reactions between rotifer-type biopolymers and human-type aggregates. This optical imaging-based method has a history in biomarker research [23], but this is the first time, that it was applied for investigating the interacting effect of biopolymers.

The H-A $\beta$  containing deposits or plaques can be detected by various absorbent (e.g., Congo red) or fluorescent dyes (e.g., Thioflavin S, Thioflavin T/ThT/, ANS or Bis-ANS). Among methods (e.g., mass spectrometry or infrared spectroscopy), analyzing molecular interaction, the efficacy of the anti-amyloid compounds *in vitro* can be semi-quantified by detecting the relative fluorescence intensity of the above-mentioned dyes [24] in targeted biochemical samples. Functional fluorophores with different specificity can be selected depending on the type of A $\beta$ s and the aim of the related experiments. The aggregates, as targets with various size and profiles, bind to dyes in diverse extents. The Bis-ANS is better able to detect the oligomer-type of H-A $\beta$  than the fibrils with a larger conformational spectrum. The ThT binds with higher affinity to H-A $\beta$  fibrils than to oligomers, based on the beta-sheet structure preference [24,25].

Based on the previously published facts [21,22] as well as on the novelties of the current research, the Rotimer has a high potential of becoming a promising drug candidate for human application in pharmacology and clinical medicine.

## 2. Materials and methods

### 2.1. Materials

Materials applied in this work were the following: yeast (*Saccharomyces cerevisiae*; EU-standard granulated instant form, cat. no.: 2-01-420674/001-Z12180/HU); algae (*Chlorella vulgaris*; BioMenu, Caleido IT-Outsource Kft.; cat. no.:18255); the applied fluorescent dyes were obtained from Sigma-Aldrich: 4,4'-dianilino-1,1'-binaphthyl-5,5'-disulfonic acid dipotassium salt (Bis-ANS, cat. no.: D4162) and Thioflavin T (ThT; cat. no.: T3516); from Merck: distilled water (DW; Millipore Ultrapure); from Life Technologies AS: DynaMag-2 magnet (cat. no.: 12321D); Dynabeads M-270 superparamagnetic epoxy beads (cat. no.: 14301); from Greiner: 96-well microplate with half-area (cat. no.: 675101, Greiner Bio-One International); from Corning: treated (cat. no.: 430293) and non-treated (cat. no.: 430591) Petri dishes, culture flasks (cat. no.: 430168); Whatman filter with 10  $\mu$ m diameter pore (cat. no.: 6728-5100); universal plastic web (pore diameter: 50  $\mu$ m); the amount of diluted cations and anions in standard medium (mg/L): Ca<sup>2+</sup> 30; Mg<sup>2+</sup> 15; Na<sup>+</sup> 3.2; K<sup>+</sup> 0.5; HCO<sub>3</sub><sup>-</sup> 150; SO<sub>4</sub><sup>-</sup> 2.5; Cl<sup>-</sup> 1.4; NO<sub>3</sub><sup>-</sup> 4.5; F<sup>-</sup> 0.01; SiO<sub>2</sub> 8; pH = 7.5; conductivity (20 °C): 428  $\mu$ S/cm. Human-type beta-amyloid 1-42 (H-A $\beta$ ; cat. no.: A14075, human Amyloid b-Peptide 1-42; cat. no.: 107761-42-2) was purchased from AduoQ Bioscience LLC., California. The scrambled A $\beta$  (S-A $\beta$ ) (LKAFDIGVEYNKVGEGFAISHGVAHLDVDMSFMFGIGRVDVHQA) were prepared at the Department of Medical Chemistry, University of Szeged, Szeged, Hungary. The peptides were synthesized on an Fmoc-Ala-Wang resin using N $\alpha$ -Fmoc-protected amino acids with a CEM Liberty microwave peptide synthesizer (Mathews, NC, USA).

### 2.2. Preparation of the amyloid aggregates

The concentrations of the various beta-amyloid (H-A $\beta$  and S-A $\beta$ ) stock solutions were 1 mg/mL in DW. The aggregation time was 3 h (3 h) or 3 days (3d) alone or together with Rotimer Inductor Conglomerate (RIC) at 24 °C (pH 3.5). The neutralization (to pH 7.5) was performed with NaOH (1 N) [26]. At the end of the aggregation process the samples were vortexed (5 min; 600 rpm) and before using their stock solutions, they were ultrasonicated (Emmi-40 HC, EMAG AG, Mörfelden-Walldorf, Germany) for 10 min at 45 kHz to achieve semi-sterilization and homogenization. After 20-fold dilution with standard medium, the final concentration of A $\beta$ s were 50  $\mu$ g/mL.

### 2.3. Animal culture

The experiments were performed on *E. dilatata* and *L. bulla* monogonant rotifer species; therefore, no specific ethical permission was needed according to the current international regulations. The species have been maintained and cultured at standard laboratory conditions for several years. These parameters and the origin of the above-mentioned rotifers were precisely described previously by Datki et al. [22]. For standard food of cultures, a mixture of homogenized baker's yeast and alga was used after heat-inactivation and filtration (diameter of particles ranged 8–10  $\mu\text{m}$ ).

### 2.4. Rotimer induction, RIC production and harvesting

As a first step, monogonant populations ( $1200 \pm 85$  individuals) were harvested from the culturing flasks by selective accumulation of animals with a plastic web (pore size 50  $\mu\text{m}$ ) into surface-treated Petri dishes (55  $\text{cm}^2$  area). The animals were currently unfed, their stomachs were empty by the second day following feeding. This precaution was necessary to avoid contamination of RIC-solution with their faeces.

The inductor (epoxy-metal beads; 200  $\mu\text{L}$  vortexed stock solution with a dose of 6  $\text{mg/mL}$  concentration) of Rotimer secretion was added to the rotifer-containing standard medium (30 mL in Petri dishes) for 2 h. Based on the manufacturer's product description of the Dynabeads M-270, 1 mg of these beads can bind approximately  $10 \pm 2$   $\mu\text{g}$  of ligands (in this case the Rotimer); however, 6 mg of beads from one induction can theoretically bind about 50–60  $\mu\text{g}$  Rotimer onto their surfaces if they are

widely covered. Calculating with this amount of biopolymer, the working concentration of A $\beta$ s was determined to be 50  $\mu\text{g/mL}$ . The RIC productions by rotifers were monitored under light microscope (at 63 $\times$  magnification; Leitz Labovert FS, Wetzlar, Germany). The attachment of Rotimer onto the epoxy beads was validated by scanning electron microscopy which was presented in our previous publication [22].

In order to perform all types of measurements in this work, RIC samples were prepared in a newly modified version compared to previous studies. The medium, including animals in Petri dishes, was removed repetitively and carefully by a pipette (5 mL working volume) then, the Rotimer-containing RIC were mechanically recovered and homogenized in 5 mL DW. The remaining rotifers were removed by filtration using the above-mentioned plastic web. The animal-free, but RIC-containing solution was then prepared at room temperature, applying DynaMag-2 magnet to fix the exudate-coated beads temporarily and reversibly. The supernatant was removed by a pipette and the RIC-pellet was washed once with DW and finally resuspended in 150  $\mu\text{L}$  DW. This conglomerate material solution was used for all types of measurements.

### 2.5. RIC-A $\beta$ interaction protocols

#### 2.5.1. Stagogram-based optical assay

After a short time (5 min) of incubation, the interaction between mixed monogonant-specific RIC (6 mg Rotimer-coated epoxy beads per mL) and 3 h or 3d A $\beta$  aggregates were investigated. The beads were isolated with a magnet in the previously described way. After discarding

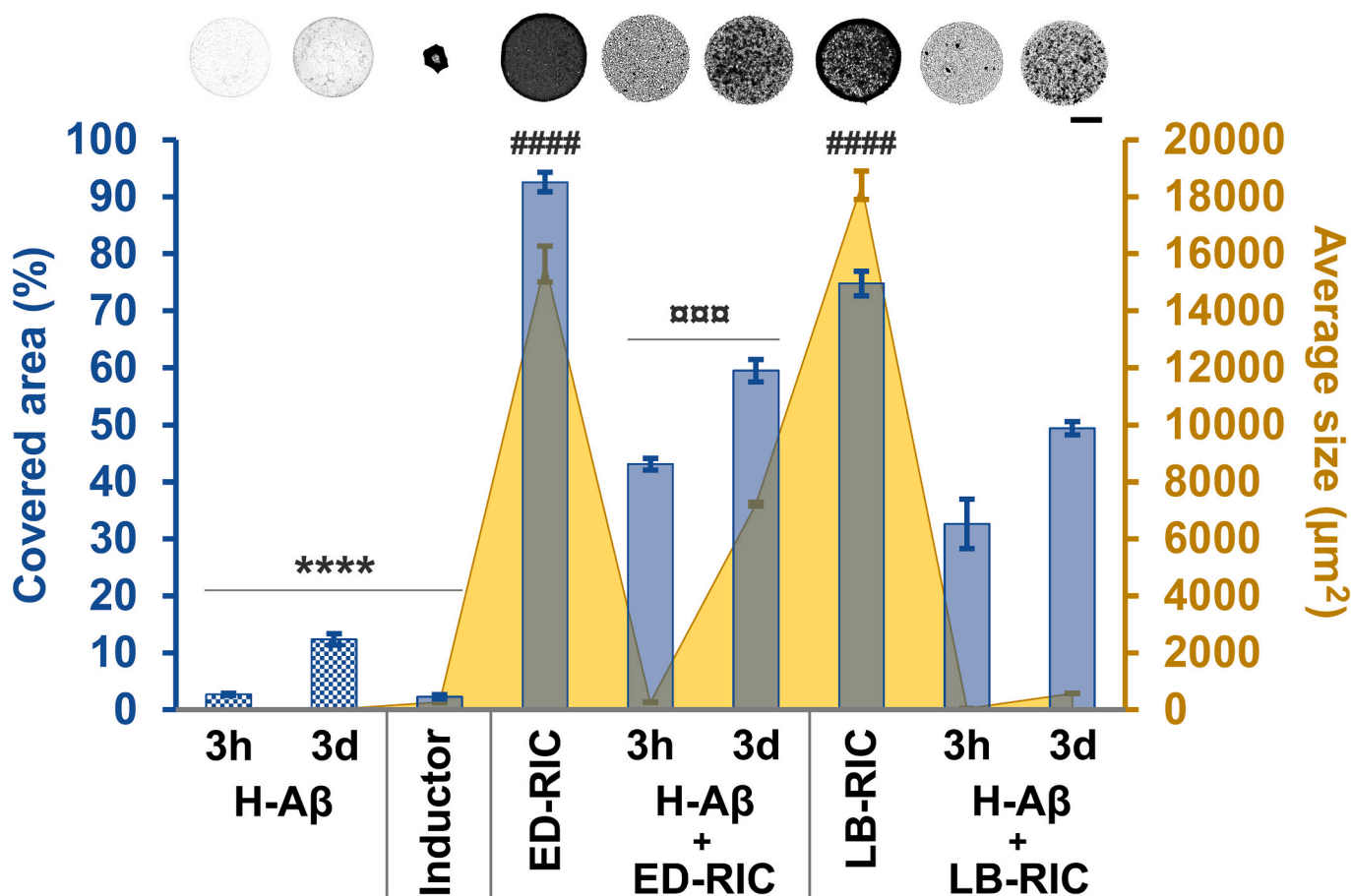


**Fig. 1.** Stagogram-based optical imaging and analysis of RIC and aggregated H-A $\beta$  interactions. ED: *Euchlanis dilatata*; LB: *Lecane bulla*; RIC: Rotimer Inductor Conglomerate; H-A $\beta$ : human-type beta-amyloid 1-42; Scale bar represents 0.5 mm. The error bars represent SEM. One-way ANOVA with Bonferroni *post hoc* test was used for statistical analysis, the levels of significance are  $p^{****} \leq 0.0001$  or  $p^{####} \leq 0.0001$  (\*, significant difference from all other groups; #, significant difference from those treated with the same ED-RIC; □, significant difference from LB-RIC belonging to the same group).

the supernatant, the pellet was washed and resuspended in 150  $\mu\text{L}$  DW. Drops ( $n = 10$ ) with 1  $\mu\text{L}$  volume were put onto non-treated hydrophobic plastic surface of Petri dish, then, they were dried for 1 h at 40% humidity.

The formed stagograms of the drops (Fig. 1) were detected by light microscopy and were photographed (Nikon D5600, 25 MP, RAW/NEF, 14 bit; Nikon Corp., Kanagawa, Japan). The digital pictures were converted into a black and white graphical format with greyscale (threshold; 2.46 pixel = 1  $\mu\text{m}$ ; 8-bit). Maximum measured area of the drops was 1.68  $\text{mm}^2$ . These images (total area of this complex) were analyzed with ImageJ program (Wayne Rasband, USA) and the related extracting data of the conglomerate-covered area (%) and the average size ( $\mu\text{m}^2$ ) were presented.

2.5.2. Bis-ANS- and ThT-based fluorescent assays

The amyloid-sensitive Bis-ANS and ThT dyes were applied in fluorescent-based *in vitro* (animal-free) experiments ( $n = 12$  wells/sample type) including investigations on: quick molecular interaction (Fig. 2) and on anti-aggregation (Fig. 3A) or disaggregation (Fig. 3B). The final dose of the dyes was 50  $\mu\text{M}$ .

In these interaction-specific experiments, the 3 h or 3d A $\beta$  aggregates

(final concentration 50  $\mu\text{g}/\text{mL}$ ) were mixed with RIC (6 mg epoxy beads/mL), similarly to the stagogram protocol, where the incubation time was only 5 min. The free A $\beta$ -containing supernatants and the RIC-A $\beta$  pellets were measured separately. Bis-ANS was used for 3 h samples, while ThT was preferred in the case of 3d ones. In the anti-aggregation study, the H-A $\beta$ -stock solution (1 mg/mL) and the concentrated RIC (120 mg epoxy/mL) were incubated together during the whole aggregating period (3d). The H-A $\beta$  and RIC stock solutions were also incubated together for 12 h and the measurements were also performed in the case of disaggregation experiments. In these cases, the Rotimer containing RIC-A $\beta$  mixes were not separated to pellet and supernatant, their fluorescent intensity was recorded together by applying the fluorescent dyes alternately. The dose ratio of A $\beta$ s and the theoretically calculated Rotimer was 1:1 in each study.

Samples containing the investigated molecules were measured with a BMG NOVostar micro-plate reader (BMG Labtech, Ortenberg, Germany) at ex/em: 405/520 nm on Bis-ANS and 450/480 nm on ThT, using a 96-well plate with half well area (100  $\mu\text{L}/\text{well}$ ). The number of laser flashes per well was 30 and orbital shaking (3 s and 600 rpm) was applied before each detection. Calibration/gain adjustment was 1% of the maximal relative intensity, where the blank of the relevant

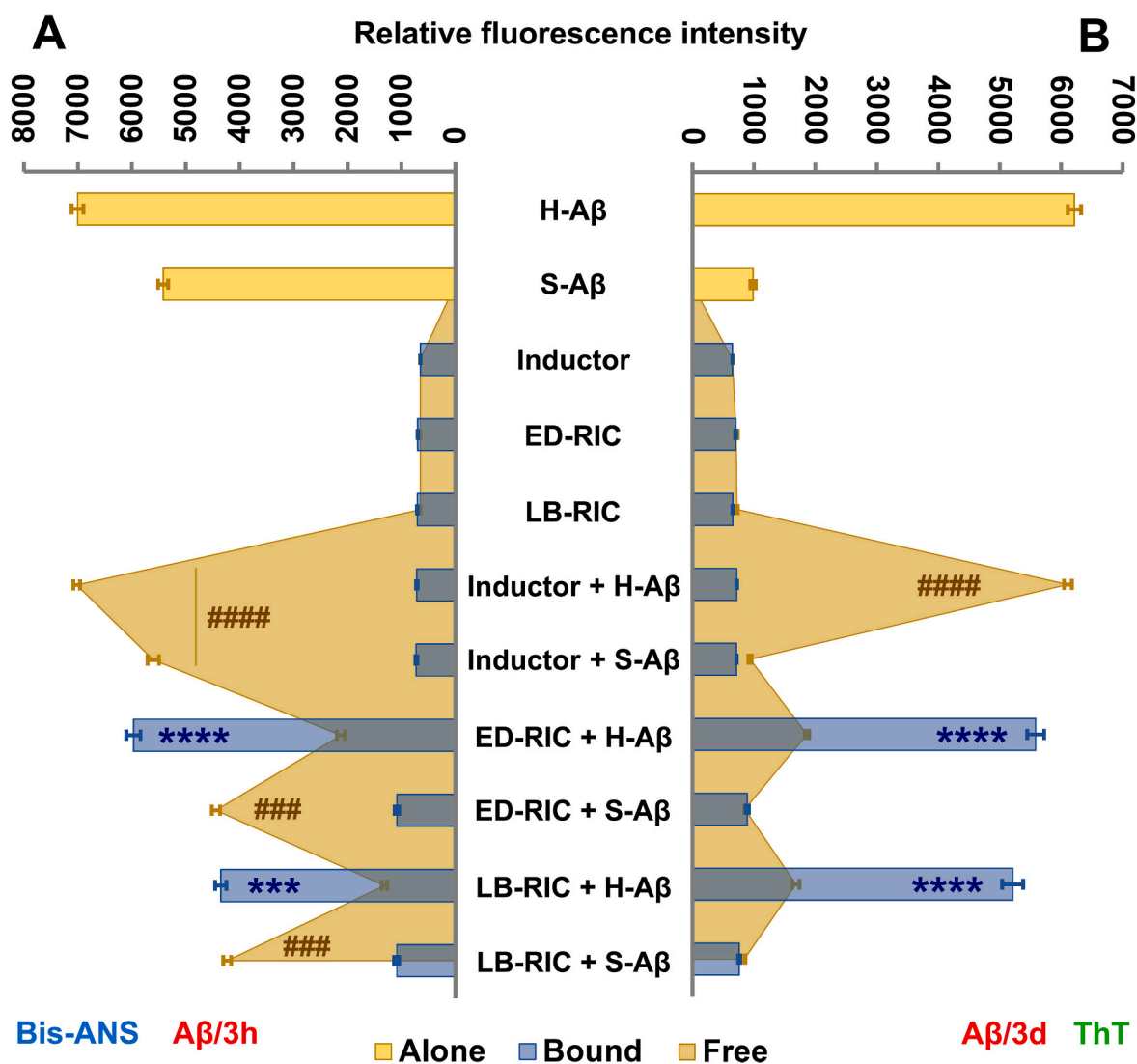
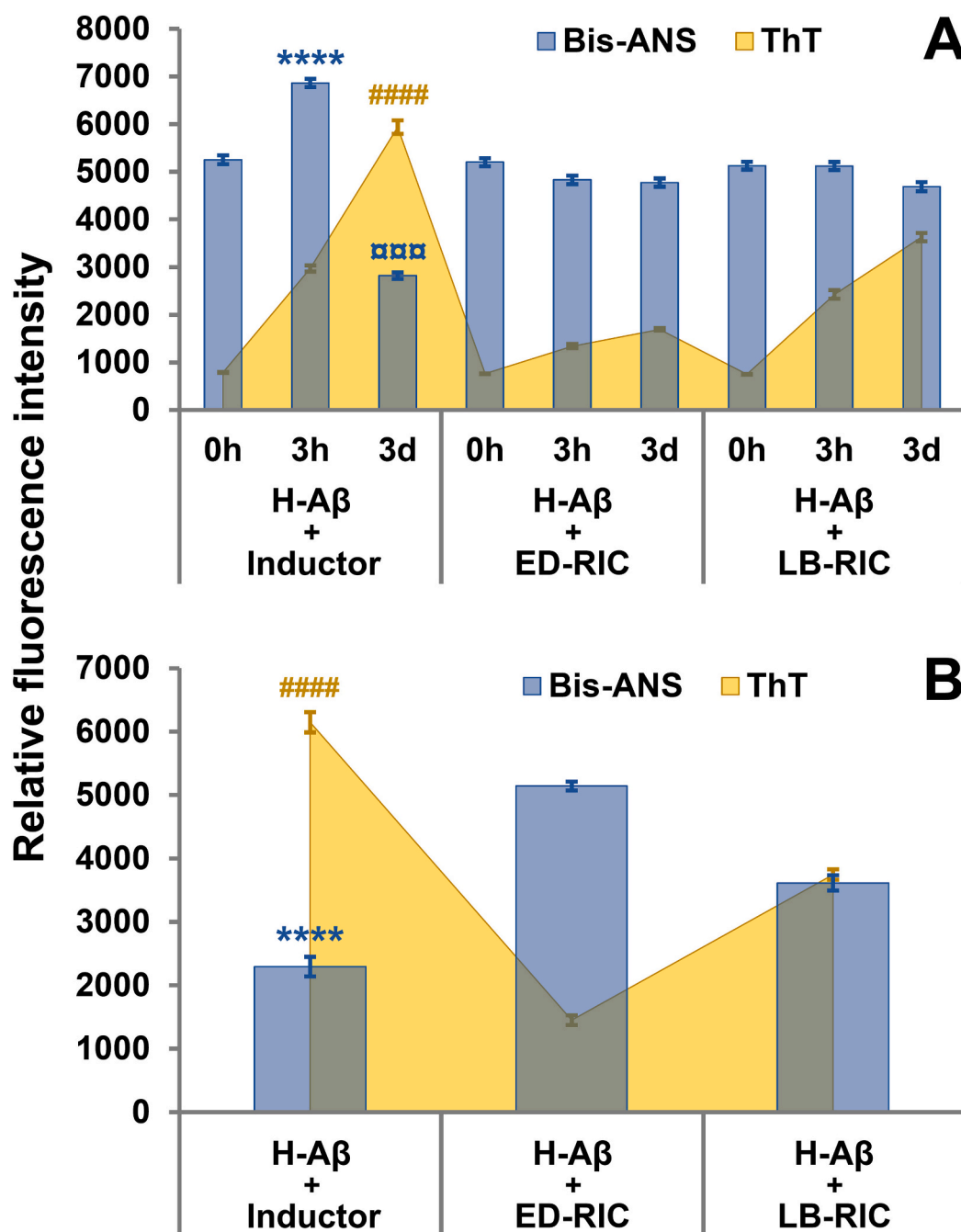


Fig. 2. Quick and sequence-based interaction of *E. dilatata*- and *L. bulla*-specific RIC with H-A $\beta$  aggregates (3 h and 3d). ED: *Euchlanis dilatata*; LB: *Lecane bulla*; RIC: Rotimer Inductor Conglomerate; H-A $\beta$ : human-type beta-amyloid 1-42. The error bars represent SEM. One-way ANOVA with Bonferroni *post hoc* test was used for statistical analysis, the levels of significance are  $p^{****,###} \leq 0.001$  or  $p^{****,####} \leq 0.0001$  (\*, significant difference from all other bound-type groups; #, significant difference from all other free-type inductor, RIC and RIC + H-A $\beta$  groups).





**Fig. 3.** Anti-aggregation (A) and disaggregation (B) effects of *E. dilatata*- and *L. bulla*-specific RIC against H-A $\beta$  aggregates (3 h and 3d). ED: *Euchlanis dilatata*; LB: *Lecane bulla*; RIC: Rotimer Inductor Conglomerate; H-A $\beta$ : human-type beta-amyloid 1-42. The error bars represent SEM. One-way ANOVA with Bonferroni *post hoc* test was used for statistical analysis, the levels of significance are  $p^{****} \leq 0.001$  or  $p^{****} \leq 0.0001$  (\*, significant difference from all other Bis-ANS groups; #, significant difference from all other ThT groups; □, significant difference from RIC-containing 3d Bis-ANS group).

fluorescent dye was about 650. The labelling time of the samples with the dyes took 5 min before starting detection.

## 2.6. Statistics

Statistical analysis was performed with SPSS 23.0 (SPSS Inc., USA) using one-way ANOVA with Bonferroni *post hoc* test. The error bars represent the standard error of the mean (SEM). The homogeneity and normality of the data were checked, and they were found suitable for ANOVA followed by Bonferroni *post hoc* test. Using the above-mentioned statistical test, 99% confidence level (1-alpha, alpha = 0.01) was applied and 1% error was handled in this analysis. The different levels of significance are indicated as follows:  $p^{***}, ###, **** \leq 0.001$  and  $p^{****}, #### \leq 0.0001$ . All relations and comparisons between the presented groups are defined in the given figure legend.

## 3. Results and discussion

The investigation of function, nature and applicability of biopolymers is a significant branch of biology nowadays [27]. The list of these natural and multifunctional materials is long; moreover, all of them have unique characteristics, making it necessary to study them individually. Such a relevant material is the recently published rotifer-specific biopolymer, namely Rotimer [22]. This biomolecule is a species-specific exudate of the relevant micrometazoa. *E. dilatata* and *L. bulla* monogonants are prominent representatives of the exogenic fiber-producing animals.

This current study has two objectives: on one hand to investigate the binding between the biopolymer-containing conglomerates and H-A $\beta$  neurotoxic aggregates and, on the other hand, to reveal the effects of RIC complex on H-A $\beta$  aggregation itself. The measurements could not be

carried out with Rotimer lacking an inductor material (epoxy-metal beads), because according to our current knowledge and empirical experience, there is no method available to remove the mentioned biomolecule from the inductor without any structural changes (e.g., a chemical one, such as racemization in alkaline solution). The organizing conditions and the binding of aggregates were monitored directly and indirectly with optical imaging methods; however, the detailed investigation of physicochemical properties was beyond the scope of this paper. RIC is the only possible form used for empirical characterization [28] and treatment studies at the time of this current publication.

Presumably, the Rotimer plays an outstanding role in the neurotoxic aggregates-catabolism caused by rotifers [21]; therefore, it is reasonable to study this exceptional phenomenon. As a first step, the quick interaction (taking a few minutes) between the natural polymers of rotifers and the artificially made H-A $\beta$  was investigated, applying two different methods. The binding between H-A $\beta$  and *E. dilatata*- or *L. bulla*-RIC (ED/LB-RIC) was measured by the so-called stagogram analysis (Fig. 1), which is a simple, but widely accepted method to visualize, for instance, the aggregation capacity of the different molecular composition of samples, based on their optical diversity [23,29]. This technique is a sensitive crystallizing process using the covered (%) area and average size ( $\mu\text{m}^2$ ) parameters of particles. These indicators can be adequately applied during the image analysis, based on the number and size of the conglomerate unit; moreover, the dried drops can be qualitatively differentiated. Differently treated groups were investigated and compared with the adequate controls. The effective agent in the present case was the RIC (epoxy beads with Rotimer).

The A $\beta$ s were aggregated for 3 h (3 h) or for three days (3d) before mixing them with the respective RIC. Then, we measured the inductor itself, H-A $\beta$  and ED/LB-RIC alone, and the conglomerates of H-A $\beta$  with the ED/LB-RIC respectively, using the stagogram based optical assay (Fig. 1). The solutions of fresh (0 min) H-A $\beta$  and S-A $\beta$  (with a random sequence of amino acids) were not presented on the stagogram figure, because they showed transparent crystallizing patterns; therefore, the borders of the dried samples could not be identified.

The crystallized drops of the groups were different both in their density and structure phenotype (Fig. 1). This is a closed and precisely defined chemical environment with few components; however, it is a well controllable *in vitro* system. The profiles of the different samples represent the interactions between the components during crystallization. The presence, absence, or variations in the amounts of determining factors is the quintessence of this drying process. According to the optical stagogram markers, the parameters of H-A $\beta$ , the inductor and the conglomerates significantly differed from each other. The more aggregated (3d) H-A $\beta$  showed a denser pattern compared to the ones incubated for a few hours (3 h). Both RIC groups of the two tested rotifers presented outstanding density in the empiric analysis of stagograms; therefore, they provided maximal reference to further analyze other samples. After removing the unbound/free H-A $\beta$ , it can be noted that the biopolymers of the two species bind to aggregates; furthermore, the optical density of relevant stagograms, derived from RIC alone, decreased in the presence of H-A $\beta$  in the conglomerate. We observed a higher level of density of the ED-RIC/H-A $\beta$  conglomerate compared to the LB-RIC/H-A $\beta$  ones. Based on the results, it can be stated that there are possible molecular interactions between the Rotimer and A $\beta$ s, particularly with the H-A $\beta$  form. The relations between RIC and H-A $\beta$  of both rotifer species showed similar tendencies; however, we also noticed that the pictures were significantly brighter of the samples originating from *L. bulla*.

Besides and parallel with the optical analysis, the quick interactions between the molecules of interest were investigated by fluorescent methods. To measure the fluorescent indicator signals, two adequate dyes were applied, the Bis-ANS and the ThT. According to literature, these molecules have different binding affinities to various aggregates [30]. These functional sensors can mark the oligomeric and fibrillar forms of A $\beta$ s, labeling the whole conformational spectrum of H-A $\beta$ s. The

Bis-ANS is more sensitive to the oligomers [24], while the ThT is more adequate for the fibrils [25,31]. Based on the previous A $\beta$  characterizations [21,32–34], it can be stated that the 3 h and 3d aggregating periods are well-reflected for the larger quantity of the oligomers or fibrils in the relevant samples. The H-A $\beta$  (3 h) with lower organization contains oligomers in higher proportions, and they were measured by Bis-ANS, while the considered fibrillar ones with longer incubation time (3d) were detected by ThT (Fig. 2). All samples were monitored with both fluorophores in anti- (Fig. 3A) and disaggregating (Fig. 3B) measurements.

The results of the interaction studies (Fig. 2) can be classified into three units: 1. H-A $\beta$ -types alone; 2. inductor, various RIC-versions and the inductor-A $\beta$  interactions as appropriate controls; 3. the connections between the species-specific RIC and the various H-A $\beta$ s (according to amino acid sequence and levels of aggregation). Based on the applied aggregates, three categories can be identified: 1. A $\beta$ s alone; 2. free A $\beta$ s in the supernatant; 3. binding A $\beta$ s to the RIC-types.

The given forms of H-A $\beta$  aggregates showed elevated fluorescence intensities in the presence of both Bis-ANS and ThT, in contrast with S-A $\beta$ , which shows higher signal intensity rather together with Bis-ANS. The S-A $\beta$  with random sequence presented decreased aggregating organization. Measurements of the A $\beta$ s alone were the reference points for further experiments. The relevant fluorescence intensities of the inductor and ED/LB-RIC combinations were also measured and used as a background control to the aspecific binding. Based on the achieved results it can be concluded that they show a minimal binding between the above-mentioned reference controls and the applied fluorescent dyes during the relatively short incubation time. Besides these cutoff values, the binding of A $\beta$ s to biopolymer-containing RIC was significantly measurable. Here, the inductor alone was not a disturbing factor either. After removing the non-bound (free) A $\beta$ s with supernatant, the binding of aggregates to RIC were labeled. The H-A $\beta$  interacted with the conglomerates of both rotifer species, and a relatively high fluorescent signal was shown, while the S-A $\beta$  had a lower value similarly to the background control. The data derived from this reference amyloid type led us to conclude sequence specificity in H-A $\beta$ -binding to biopolymers. In our previous publication [35], the sequence-specific effect of H-A $\beta$  was proved in the autotaxolism-related processes of rotifers compared to S-A $\beta$ . The H-A $\beta$  samples with lower (3 h) or higher (3d) conformational organization were significantly bound to both tested Rotimer coatings, but they showed higher affinity to the biopolymer secreted by *E. dilatata* than the one produced by *L. bulla*.

After proving the particular interaction between Rotimer and H-A $\beta$ , the effects of the investigated biopolymer on aggregation processes were tested using Bis-ANS and ThT measurements, which were able to indirectly detect the approximate aggregation status of A $\beta$ s. The controls showed similar fluorescence intensity to the previously measured ones (Fig. 2); therefore, they were not presented again in this case. To measure the anti-aggregating effects of RIC-types (Fig. 3A), H-A $\beta$  was applied with various aggregation times (0 h, 3 h and 3d). During co-incubation, the inductor alone did not inhibit the aggregation of H-A $\beta$ ; however, the initial signal of Bis-ANS significantly decreased in the 3d sample, while the ThT signal increased. These results refer to the time-dependent high aggregation level of H-A $\beta$ ; moreover, these processes are in line with the relevant literature [36,37]. In contrast with the above mentioned, the H-A $\beta$  (3 h and 3d) + RIC related ThT signals decreased in samples of both relevant species, while the Bis-ANS fluorescence remained on the reference (0 min) level. The materials from *E. dilatata* proved to be more effective in anti-aggregation processes than the ones derived from *L. bulla* applying the same experimental period of time. The 3d group showed the less efficiency. In the LB-RIC and H-A $\beta$ /3d combination, the ThT resulted an elevated level; thus, unlike in the other samples, there was no clear conclusion about the aggregation changes of H-A $\beta$ .

The following experiments revealed that the presence of the inductor alone during a further 12 h had no impact on the condition of 3d-pre-

aggregated H-A $\beta$  (Fig. 3B). In these cases, the Bis-ANS and ThT signal ranges are alike the previously presented data (Fig. 3A). In contrast, the control Bis-ANS and ThT values significantly differed from the RIC-containing ones from the same category at the end of disaggregating processes. During the co-incubation time, the RIC of both monogonant species increased the level of Bis-ANS sensitive oligomers, and they decreased the concentration of ThT-specific fibrillar forms. Based on the characteristics of the two fluorophores it may be assumed that the presence of Rotimer in the samples has a disaggregating effect against the H-A $\beta$ . Such as in the previous measurements, the biopolymer of *E. dilatata* was more efficient, and it gave more comprehensible results about the condition of the neurotoxic aggregates.

Different behavior of RIC-types on H-A $\beta$ -binding and aggregating processes, derived from the two different species, can be further explained. One interpretation may be that *L. bulla* originally secreted less biopolymer to the epoxy beads than *E. dilatata*. Another possibility is that the biopolymers may differ in the various rotifer species in terms of structure, functionality, and efficacy. The anti-aggregation effect of LB-RIC did not increase when the number of animals was higher during longer secretion time (4 h) of Rotimer, or a two-fold dose of RIC was tested in the presence of standard H-A $\beta$  amount (data not shown).

Altogether, the results show that the ED/LB-RIC, with proteinous exudate on their surface, explicitly binds the H-A $\beta$ . It is an efficient influencing factor in aggregation kinetics; moreover, the activity of the species-specific biopolymers may differ from each other. Further proteomic experiments (e.g., mass spectrometry) are needed to investigate the interaction between the Rotimer and the neurotoxic protein aggregates (e.g., alpha-synuclein and prions). It is well-known that during the Rotimer secretion, the calcium is built-in [28], and it may provide different ionic characteristics to this biomaterial; therefore, the metal ion content of the biopolymer may enhance these molecular relations. The mechanism of anti- and disaggregating ability may be similar to the action of beta-sheet-breaker molecules or that of some natural (LPFFD, [38]; RIIGL, [39–41]) or artificial (LPYFD, [32,42]) peptide sequences. The spectroscopic analysis of Rotimer may give the proper answer to these questions, which will be part of the following projects.

In summary, it is essential to highlight that the direct molecular effects of natural polymers [43,44] on neurodegeneration-related amyloids have been barely investigated, resulting only a few cases [13]. Based on the results obtained, Rotimer is assumed to have a structure-breaking capability, dissociating H-A $\beta$  aggregates. The current rotifer-specific biomaterials, namely Rotimers, were used for that purpose for the first time. Concerning the protective role of Rotimer against H-A $\beta$ , indirect *in vivo* measurements were carried out [22]; however, *in vitro* binding, anti- and disaggregating experiments have never been previously performed. Moreover, this interdisciplinary approach may also open novel perspectives in pharmacological research against Alzheimer's disease.

#### 4. Conclusion

Various interactions were discovered between human-type amyloids and other biological and synthetic drugs, e.g., antibodies, hormones, polymers, or small molecules. The present work aimed to measure the binding interaction between the Rotimer-containing conglomerate (formed by rotifers) and neurotoxic H-A $\beta$  peptide aggregates; moreover, to investigate the effect of this RIC on A $\beta$  aggregation processes. To prove these, two test methods were used, namely optical stagogram and fluorescence intensity measurement. The obtained results reflect the relationship between RIC and H-A $\beta$ , in addition, the stable interaction shows A $\beta$  sequence specificity. There was minimal binding between RIC and S-A $\beta$ . The conglomerate of both monogonant rotifer species (*E. dilatata* and *L. bulla*) interacted with H-A $\beta$  considered as oligomer and/or fibril type; however, ED-RIC was more effective in binding and aggregation processes. The novelty of this work is the first demonstration of the *in vitro* interaction between Rotimer and H-A $\beta$  by presenting

the anti- and disaggregating effects of this biopolymer against the neurotoxic agents of AD. Due to its properties mentioned above, this natural material needs further study in the future; moreover, this biopolymer can be a relevant molecular specimen for developing drug candidates in neurodegeneration-related research.

#### Ethical approval

All applicable international, national, and/or institutional guidelines for the care and use of animals were followed. Our experiments were performed on rotifers; therefore, according to the current ethical regulations, no specific ethical permission was needed. The investigations were carried out in accordance with globally accepted norms: Animals (Scientific Procedures) Act, 1986, associated guidelines, EU Directive 2010/63/EU for animal experiments and the National Institutes of Health guide for the care and use of Laboratory animals (NIH Publications No. 8023, revised 1978). Our animal studies comply with the ARRIVE guidelines.

#### Availability of data and material

The datasets used and/or analyzed during the current study available from the corresponding author on reasonable request.

#### Funding

This project was supported by the János Bolyai Research Scholarship of the Hungarian Academy of Sciences; by the UNKP-21-5-SZTE-555 New National Excellence Program of the Ministry for Innovation and Technology from the source of the National Research, Development and Innovation Found; by the European Union's Horizon 2020 research and innovation programme under the Marie Skłodowska-Curie grant agreement, Nr. 754432; by the Polish Ministry of Science and Higher Education; by the SZTE ÁOK-KKA No. 5S 567 (A202) and by the Developing Scientific Workshops of Medical-, Health Sciences and Pharmaceutical Training (grant number: EFOP 3.6.3-VEKOP-16-2017-00009; Hungary).

#### CRediT authorship contribution statement

Zsolt Datki: Investigation, Formal analysis, Writing- Original draft preparation, Visualization, Funding acquisition, Project administration. Evelin Balazs: Visualization, Writing- Original draft preparation, Funding acquisition. Bence Galik: Software, Data Curation, Funding acquisition. Lavinia Zeitler: Methodology, Visualization. Janos Kalman: Conceptualization, Resources. Rita Sinka: Resources, Writing-Reviewing and Editing. Zsolt Bozso: Methodology, Resources. Tibor Hortobagyi: Resources, Writing - Review & Editing, Funding acquisition. Zita Galik-Olah: Validation, Writing - Review & Editing, Project administration.

#### Declaration of competing interest

The authors declare that they have no competing interests.

#### Acknowledgements

The authors wish to thank to Anna Szentgyorgyi MA, a professional in English Foreign Language Teaching for proofreading the manuscript.

#### References

- [1] H. Chi, H.Y. Chang, T.K. Sang, Neuronal cell death mechanisms in major neurodegenerative diseases, *Int. J. Mol. Sci.* 19 (2018) 1–18, <https://doi.org/10.3390/ijms19103082>.
- [2] J.R. Backstrom, G.P. Lim, M.J. Cullen, Z.A. Tökés, Matrix Metalloproteinase-9 (MMP-9) is synthesized in neurons of the human hippocampus and is capable of

- degrading the amyloid-peptide (1–40), *J. Neurosci.* 16 (24) (1996) 7910–7919, <https://doi.org/10.1523/JNEUROSCI.16-24-07910.1996>.
- [3] C.A. Ross, M.A. Poirier, Protein aggregation and neurodegenerative disease, *Nat. Med.* 10 (2004) S10–S17, <https://doi.org/10.1038/nm1066>.
- [4] R.J. Baranello, K.L. Bharani, V. Padmaraju, N. Chopra, D.K. Lahiri, N.H. Greig, M. A. Pappolla, K. Sambamurti, Amyloid-Beta protein clearance and degradation (ABCD) pathways and their role in Alzheimer's disease, *Curr. Alzheimer Res.* 12 (2015) 32–46, <https://doi.org/10.2174/1567205012666141218140953>.
- [5] V. Kumar, N. Sami, T. Kashav, A. Islam, F. Ahmad, M.I. Hassan, Protein aggregation and neurodegenerative diseases: from theory to therapy, *Eur. J. Med. Chem.* 124 (2016) 1105–1120, <https://doi.org/10.1016/j.ejmech.2016.07.054>.
- [6] B. Vellas, N. Coley, P.J. Ousset, G. Berrut, J.F. Dartigues, B. Dubois, H. Grandjean, F. Pasquier, F. Piette, P. Robert, J. Touchon, P. Garnier, H. Mathiex-Fortunet, S. Andrieu, Long-term use of standardised ginkgo biloba extract for the prevention of Alzheimer's disease (GuidAge): a randomised placebo-controlled trial, *Lancet Neurol.* 11 (2012) 851–859, [https://doi.org/10.1016/S1474-4422\(12\)70206-5](https://doi.org/10.1016/S1474-4422(12)70206-5).
- [7] F. Yang, G.P. Lim, A.N. Begum, O.J. Ubeda, M.R. Simmons, S.S. Ambegaokar, P. Chen, R. Kaye, C.G. Glabe, S.A. Frautschy, G.M. Cole, Curcumin inhibits formation of amyloid  $\beta$  oligomers and fibrils, binds plaques, and reduces amyloid in vivo, *J. Biol. Chem.* 280 (2005) 5892–5901, <https://doi.org/10.1074/jbc.M404751200>.
- [8] X. Le Bu, P.P.N. Rao, Y.J. Wang, Anti-amyloid aggregation activity of natural compounds: implications for Alzheimer's drug discovery, *Mol. Neurobiol.* 53 (2016) 3565–3575, <https://doi.org/10.1007/s12035-015-9301-4>.
- [9] R.H.K.M.K. Siddiqi, P. Alam, S.K. Chaturvedi, Y.E. Shahein, Mechanisms of protein aggregation and inhibition, *Front. Biosci. (Elite Ed.)* 9 (2017) 1–20, <https://doi.org/10.2741/e781>.
- [10] T. Thomas, T.G. Nadackal, K. Thomas, Aspirin and non-steroidal anti-inflammatory drugs inhibit amyloid- $\beta$  aggregation, *Neuroreport.* 12 (2001) 959–965, <https://doi.org/10.1097/00001756-200110290-00024>.
- [11] A. George, M.R. Sanjay, R. Srisuk, J. Parameswaranpillai, S. Siengchin, A comprehensive review on chemical properties and applications of biopolymers and their composites, *Int. J. Biol. Macromol.* 154 (2020) 329–338, <https://doi.org/10.1016/j.ijbiomac.2020.03.120>.
- [12] K.J. Wilkinson, A. Joz-Roland, J. Bufjee, Different roles of pedogenic fulvic acids and aquagenic biopolymers on colloid aggregation and stability in freshwaters, *Limnol. Oceanogr.* 42 (1997) 7–14, <https://doi.org/10.4319/lo.1997.42.8.1714>.
- [13] B. Meesaragandla, S. Karanth, U. Janke, M. Delcea, Biopolymer-coated gold nanoparticles inhibit human insulin amyloid fibrillation, *Sci. Rep.* 10 (2020) 1–14, <https://doi.org/10.1038/s41598-020-64010-7>.
- [14] L.S. Bezerra, M. Magnani, R.J.H. Castro-Gomez, H.C. Cavalcante, T.A.F. da Silva, R. L.P. Vieira, I.A. de Medeiros, R.C. Veras, Modulation of vascular function and anti-aggregation effect induced by (1  $\rightarrow$  3) (1  $\rightarrow$  6)- $\beta$ -D-glucan of *Saccharomyces cerevisiae* and its carboxymethylated derivative in rats, *Pharmacol. Rep.* 69 (2017) 448–455, <https://doi.org/10.1016/j.pharep.2017.01.002>.
- [15] S.G. Roman, N.A. Chebotareva, B.I. Kurzanov, Anti-aggregation activity of small heat shock proteins under crowded conditions, *Int. J. Biol. Macromol.* 100 (2017) 97–103, <https://doi.org/10.1016/j.ijbiomac.2016.05.080>.
- [16] S. Nagarajan, S. Radhakrishnan, S.N. Kalkura, S. Balme, P. Miele, M. Bechelany, Overview of protein-based biopolymers for biomedical application, *Macromol. Chem. Phys.* 220 (2019) 1–16, <https://doi.org/10.1002/macp.201900126>.
- [17] A.O. Elzoghby, W.M. Samy, N.A. Elgindy, Protein-based nanocarriers as promising drug and gene delivery systems, *J. Control. Release* 161 (2012) 38–49, <https://doi.org/10.1016/j.jconrel.2012.04.036>.
- [18] S.K. Nitta, K. Numata, Biopolymer-based nanoparticles for drug/gene delivery and tissue engineering, *Int. J. Mol. Sci.* 14 (2013) 1629–1654, <https://doi.org/10.3390/ijms14011629>.
- [19] S.Y. Ow, I. Bekard, D.E. Dunstan, Effect of natural biopolymers on amyloid fibril formation and morphology, *Int. J. Biol. Macromol.* 106 (2018) 30–38, <https://doi.org/10.1016/j.ijbiomac.2017.07.171>.
- [20] B. Lengerer, R. Pjeta, J. Wunderer, M. Rodrigues, R. Arbore, L. Schärer, E. Berezikov, M.W. Hess, K. Pfaller, B. Egger, S. Obwegeser, W. Salvenmoser, P. Ladurner, Biological adhesion of the flatworm macrostomum lignano relies on a duo-gland system and is mediated by a cell type-specific intermediate filament protein, *Front. Zool.* 11 (2014) 1–15, <https://doi.org/10.1186/1742-9994-11-12>.
- [21] Z. Datki, Z. Olah, T. Hortobagyi, L. Macsai, K. Zsuga, L. Fulop, Z. Bozso, B. Galik, E. Acs, A. Foldi, A. Szarvas, J. Kalman, Exceptional in vivo catabolism of neurodegeneration-related aggregates, *Zool. Lett.* 4 (2018) 1–12, <https://doi.org/10.1186/s40478-018-0507-3>.
- [22] Z. Datki, E. Acs, E. Balazs, T. Sovany, I. Csoka, K. Zsuga, J. Kalman, Z. Galik-Olah, Exogenic production of bioactive filamentous biopolymer by monogonant rotifers, *Ecotoxicol. Environ. Saf.* 208 (2021) 1–10, <https://doi.org/10.1016/j.ecoenv.2020.111666>.
- [23] J. Murube, Tear crystallization test: two centuries of history, *Ocul. Surf.* 2 (2004) 7–9, [https://doi.org/10.1016/S1542-0124\(12\)70019-8](https://doi.org/10.1016/S1542-0124(12)70019-8).
- [24] M. Yu, T.M. Ryan, S. Ellis, A.I. Bush, J.A. Triccas, P.J. Rutledge, M.H. Todd, Neuroprotective peptide-macrocyclic conjugates reveal complex structure-activity relationships in their interactions with amyloid  $\beta$ , *Metallomics* 6 (2014) 1931–1940, <https://doi.org/10.1039/c4mt00122b>.
- [25] C. Xue, T.Y. Lin, D. Chang, Z. Guo, Thioflavin T as an amyloid dye: fibril quantification, optimal concentration and effect on aggregation, *R. Soc. Open Sci.* 4 (2017) 1–12, <https://doi.org/10.1098/rsos.160696>.
- [26] A.N. Kalweit, H. Yang, J. Colitti-Klausnitzer, L. Fulöp, Z. Bozso, B. Penke, D. Manahan-Vaughan, Acute intracerebral treatment with amyloid-beta (1–42) alters the profile of neuronal oscillations that accompany LTP induction and results in impaired LTP in freely behaving rats, *Front. Behav. Neurosci.* 9 (2015) 1–16, <https://doi.org/10.3389/fnbeh.2015.00103>.
- [27] S. Mohan, O.S. Oluwafemi, N. Kalarikkal, S. Thomas, S.P. Songca, Biopolymers – application in nanoscience and nanotechnology, recent advBiopolym. (2016) 47–72, <https://doi.org/10.5772/62225>.
- [28] E. Balazs, Z. Galik-Olah, B. Galik, F. Somogyvari, J. Kalman, Z. Datki, External modulation of rotifer exudate secretion in monogonant rotifers, *Ecotoxicol. Environ. Saf.* 220 (2021) 1–8, <https://doi.org/10.1016/j.ecoenv.2021.112399>.
- [29] A. Solé, Untersuchung über die bewegung der teilchen im stagogramm und influenzstagogramm, *Kolloid-Zeitschrift* 151 (1957) 55–62, <https://doi.org/10.1007/BF01502258>.
- [30] N.D. Younan, J.H. Viles, A comparison of three fluorophores for the detection of amyloid fibers and prefibrillar oligomeric assemblies. ThT (Thioflavin T); ANS (1-Anilino-naphthalene-8-sulfonic Acid); and bisANS (4,4'-Dianilino-1,1'-binaphthyl-5,5'-disulfonic Acid), *Biochemistry* 54 (2015) 4297–4306, <https://doi.org/10.1021/acs.biochem.5b00309>.
- [31] H. Levine, Thioflavine T interaction with synthetic Alzheimer's disease beta-amyloid peptides: detection of amyloid aggregation in solution, *Protein Sci.* 2 (1993) 404–410, <https://doi.org/10.1002/pro.5560020312>.
- [32] Z. Datki, R. Papp, D. Zádori, K. Soós, L. Fülöp, A. Juhász, G. Laskay, C. Hetényi, E. Mihalik, M. Zarándi, B. Penke, In vitro model of neurotoxicity of A $\beta$  1–42 and neuroprotection by a pentapeptide: irreversible events during the first hour, *Neurobiol. Dis.* 17 (2004) 507–515, <https://doi.org/10.1016/j.nbd.2004.08.007>.
- [33] Z. Bozso, B. Penke, D. Simon, I. Laczkó, G. Juhász, V. Szegedi, Á. Kasza, K. Soós, A. Hetényi, E. Weber, H. Tóháti, M. Cséte, M. Zarándi, L. Fülöp, Controlled in situ preparation of A $\beta$ (1–42) oligomers from the isopeptide “iso-A $\beta$ (1–42)”, physicochemical and biological characterization, *Peptides* 31 (2010) 248–256, <https://doi.org/10.1016/j.peptides.2009.12.001>.
- [34] L. Fülöp, M. Zarándi, K. Soós, B. Penke, Self-assembly of Alzheimer's disease-related amyloid peptides into highly ordered nanostructures, *Nanopages* 1 (2006) 69–83, <https://doi.org/10.1556/nano.1.2006.1.3>.
- [35] E. Balazs, Z. Galik-Olah, B. Galik, Z. Bozso, J. Kalman, Z. Datki, Neurodegeneration-related beta-amyloid as autotaxin-attenuator in a micro-in vivo system, in: *IBRO Reports* 9, 2020, pp. 319–323, <https://doi.org/10.1016/j.ibro.2020.10.002>.
- [36] R. Pellarin, A. Cafisch, Interpreting the aggregation kinetics of amyloid peptides, *J. Mol. Biol.* 360 (2006) 882–892, <https://doi.org/10.1016/j.jmb.2006.05.033>.
- [37] A. Sharma, M.A. McDonald, H.B. Rose, Y.O. Chernoff, S.H. Behrens, A. S. Bommarium, Modeling amyloid aggregation kinetics: a case study with Sup35NM, *J. Phys. Chem. B* 125 (2021) 4955–4963, <https://doi.org/10.1021/acs.jpcc.0c11250>.
- [38] B.F.C. Soto, E.M. Sigurdsson, L. Morelli, R.A. Kumar, E.M. Castaño, Beta-sheet breaker peptides inhibit fibrillogenesis in a rat brain model of amyloidosis: implications for Alzheimer's therapy, *Nat. Med.* (1998) 822–826, <https://doi.org/10.1038/nm0798-822>.
- [39] L. Fülöp, M. Zarándi, Z. Datki, K. Soós, B. Penke,  $\beta$ -amyloid-derived pentapeptide RIIGL inhibits A $\beta$  1–42 aggregation and toxicity, *Biochem. Biophys. Res. Commun.* 324 (2004) 64–69, <https://doi.org/10.1016/j.bbrc.2004.09.024>.
- [40] Ü. Murvai, K. Soós, B. Penke, M.S.Z. Keller Mayer, Effect of the beta-sheet-breaker peptide LPFFD on oriented network of amyloid  $\beta$ 25–35 fibrils, *J. Mol. Recognit.* 24 (2011) 453–460, <https://doi.org/10.1002/jmr.1113>.
- [41] M.H. Viet, S.T. Ngo, N.S. Lam, M.S. Li, Inhibition of aggregation of amyloid peptides by beta-sheet breaker peptides and their binding affinity, *J. Phys. Chem. B* 115 (2011) 7433–7446, <https://doi.org/10.1021/jp1116728>.
- [42] I. Laczkó, E. Vass, K. Soós, L. Fülöp, M. Zarándi, B. Penke, Aggregation of A $\beta$ (1–42) in the presence of short peptides: conformational studies, *J. Pept. Sci.* 14 (2008) 731–741, <https://doi.org/10.1002/psc.990>.
- [43] R. Balart, D. Garcia-García, V. Fombuena, L. Quiles-Carrillo, M.P. Arrieta, Biopolymers from natural resources, *Polymers (Basel)*. 13 (2021) 1–9, <https://doi.org/10.3390/polym13152532>.
- [44] L.I. Atanase, Micellar drug delivery systems based on natural biopolymers, *Polymers (Basel)*. 13 (2021) 1–33, <https://doi.org/10.3390/polym13030477>.